J Sci Comput (2012) 51:650–682
DOI 10.1007/s10915-011-9525-z

Summation by Parts Operators for Finite Difference Approximations of Second-Derivatives with Variable Coefficients

Ken Mattsson

Received: 7 October 2010 / Revised: 23 May 2011 / Accepted: 1 August 2011 /
Published online: 3 September 2011

Abstract Finite difference operators approximating second derivatives with variable coefficients and satisfying a summation-by-parts rule have been derived for the second-, fourth- and sixth-order case by using the symbolic mathematics software Maple. The operators are based on the same norms as the corresponding approximations of the first derivative, which makes the construction of stable approximations to general multi-dimensional hyperbolic-parabolic problems straightforward.

Keywords High-order finite difference methods · Numerical stability · Second-derivatives · Variable coefficients

1 Introduction

In many applications, such as general relativity [3, 28], seismology [12, 30], oceanography [21], acoustics [2, 5, 6, 22, 29] and electromagnetics [7, 31], the underlying equations are systems of second-order hyperbolic partial differential equations. However, as pointed out in [13], with very few exceptions the equations are rewritten and solved as a system of first-order equations. There are some benefits by solving the equations on second-order form [16]. However, stability is not so easily shown for a narrow-stencil approximation of such problems. In [19] we introduced the term *narrow*, to define explicit finite difference schemes with a minimal stencil width.

Narrow-stencil approximations of second-derivatives have long been known to have good accuracy properties [19]. Narrow-stencil second-derivative summation-by-parts (SBP) operators approximating $\partial^2/\partial x^2$ were derived in [17]. In the present study we derive narrow-stencil SBP operators approximating $\partial/\partial x(b(x)\partial/\partial x)$, where $b(x) > 0$. Stability for higher-order accurate (higher than third-order) narrow-stencil finite difference approximations applicable to second-order hyperbolic systems on general curvilinear grids have never before

K. Mattsson (✉)
Uppsala University, Uppsala, Finland
e-mail: ken.mattsson@it.uu.se

been fully addressed. The main reason has been the failure of deriving narrow-stencil higher-order accurate SBP operators for variable coefficient second-derivatives.

In [19] we introduced an important relationship between the existing first- and second-derivative SBP operators, referred to as *compatibility*. The main result of that study [19] was to prove that compatibility is a necessary condition obtaining an energy estimate (i.e., proving stability) for narrow-stencil approximations of problems with a combination of mixed $(\partial^2/\partial x \partial y)$ and non-mixed $(\partial^2/\partial x^2, \partial^2/\partial y^2)$ second-derivatives. However, that study was limited to the constant coefficient case. Typical applications deal with the corresponding variable coefficient case involving combinations of mixed $\partial/\partial x(b_{12}(x, y)\partial/\partial y)$, $\partial/\partial y(b_{21}(x, y)\partial/\partial x)$ and pure $\partial/\partial x(b_{11}(x, y)\partial/\partial x)$, $\partial/\partial y(b_{22}(x, y)\partial/\partial y)$ second-derivatives with variable coefficients, such as the compressible Navier-Stokes equations [20, 24, 25] and various second-order hyperbolic systems on curvilinear grids. The main result of the present study is the derivation and construction of narrow-stencil compatible SBP operators also for the variable coefficient problem. This is the first time such finite difference operators have been presented in literature. It is imperative to use finite difference approximations that do not allow growth in time—a property termed "strict stability" [9]. The combination of narrow-stencil SBP operators and the Simultaneous Approximation Term (SAT) method [4] to implement the boundary and interface conditions [15] makes it possible to exactly mimic the continuous energy estimate and thus proving strict stability.

In Sect. 2 we introduce the SBP-SAT method for a 1-D second-order hyperbolic problem, followed by a detailed construction procedure for the compatible SBP operators. In Sect. 3 the accuracy and stability properties of the newly developed SBP operators are verified by performing numerical simulations in 1-D. In Sect. 4 we analyze a 2-D hyperbolic system on second-order form having both mixed and pure second-derivatives with variable coefficients. We show that compatibility is a necessary condition obtaining an energy estimate for narrow-stencil approximations of such problems. In Sect. 5 conclusions are drawn. The SBP operators are presented in Appendix.

2 The 1-D Problem

In the present study the focus is on deriving SBP operators for systems involving a combination of mixed and pure second-derivative terms with variable coefficients. To make the paper more clear we begin with a presentation of the SBP and SAT concepts in 1-D.

The following definitions are needed in Sect. 4, to analyze the stability properties of the new SBP operators. Let the inner product for real-valued functions $u, v \in L^2[0, 1]$ be defined by $(u, v) = \int_0^1 uva(x)dx$, $a(x) > 0$, and let the corresponding norm be $\|u\|_a^2 = (u, u)$. The domain $(0 \le x \le 1)$ is discretized using the following $N + 1$ equidistant grid points:

$$x_i = ih, \quad i = 0, 1, \ldots, N, \; h = \frac{1}{N}.$$

The approximate solution at grid point x_i is denoted v_i, and the discrete solution vector is $v^T = [v_0, v_1, \ldots, v_N]$. Similarly, we define an inner product for discrete real-valued vector functions $u, v \in \mathbf{R}^{\mathbf{N+1}}$ by $(u, v)_{H_a} = u^T HAv$, where H is diagonal and positive definite and A is the projection of $a(x)$ onto the diagonal. The corresponding norm is $\|v\|_{H_a}^2 = v^T HAv$.

Remark The matrix product HA defines a norm if and only if HA is symmetric and positive definite. This can only be guaranteed if H is a diagonal matrix (see [23] for a detailed study on this).

The following vectors will be frequently used:

$$e_0 = [1, 0, \ldots, 0]^T, \qquad e_N = [0, \ldots, 0, 1]^T. \tag{1}$$

2.1 The SBP-SAT Method

To define the SBP-SAT method, we present the following two definitions (first stated in [19]):

Definition 2.1 An explicit pth-order accurate finite difference scheme with minimal stencil width of a Cauchy problem is called a pth-order accurate narrow-stencil.

Definition 2.2 A difference operator $D_1 = H^{-1}Q$ approximating $\partial/\partial x$, using a pth-order accurate narrow-stencil, is said to be a pth-order accurate narrow-diagonal first-derivative SBP operator if H is diagonal and positive definite and $Q + Q^T = \mathrm{diag}(-1, 0, \ldots, 0, 1)$.

We say that a scheme is explicit if no linear system of equations needs to be solved to compute the difference approximation. Spatial Padé discretizations [14] are often referred to as "compact schemes." The approximation of the derivative is obtained by solving a tri- or penta-diagonal system of linear equations at every time step. Hence, if written in explicit form, Padé discretizations lead to full-difference stencils, similar to spectral discretizations.

As an example of the simple, yet powerful, SBP-SAT method, we consider the following second-order hyperbolic equation:

$$\begin{aligned} &au_{tt} = (bu_x)_x, \quad 0 \le x \le 1,\ t \ge 0,\\ &\alpha u_t - bu_x = g, \quad x = 0,\ t \ge 0,\\ &\alpha u_t + bu_x = g, \quad x = 1,\ t \ge 0,\\ &u = f_1, \qquad u_t = f_2, \quad 0 \le x \le 1,\ t = 0, \end{aligned} \tag{2}$$

where $a(x) > 0$ and $b(x) > 0$. Multiplying the first equation in (2) by u_t, integrating by parts (referred to as "the energy method") and imposing the boundary conditions lead to

$$\frac{d}{dt}\left(\|u_t\|_a + \|u_x\|_b\right) = -2\left(\alpha u_t - g\right)u_t|^{x=1} - 2\left(\alpha u_t - g\right)u_t|_{x=0}. \tag{3}$$

An energy estimate is obtained if $\alpha \ge 0$. The discrete approximation of (2) using the SBP-SAT method is

$$\begin{aligned} Av_{tt} = {} & D_1 B D_1 v - H^{-1}\tau e_0\left\{(\alpha v_t - BD_1 v)_0 - g\right\}\\ & - H^{-1}\tau e_N\left\{(\alpha v_t + BD_1 v)_N - g\right\}, \end{aligned} \tag{4}$$

where e_0 and e_N are defined in (1). (We assume the same initial conditions $v = f_1$, $v_t = f_2$ as in the continuous case.) The matrices A and B have the values of $a(x)$ and $b(x)$ injected on the diagonal.

Applying the energy method by multiplying (4) by $v_t^T H$ and adding the transpose lead to

$$\begin{aligned} \frac{d}{dt}\left(\|v_t\|_{H_a}^2 + \|D_1 v\|_{H_b}^2\right) = {} & -(v_t)_0^T(2 - 2\tau)(BD_1 v)_0 + (v_t)_N^T(2 - 2\tau)(BD_1 v)_N\\ & + 2\tau\left(v_t^T(g - \alpha v_t)\right)_0 + 2\tau\left(v_t^T(g - \alpha v_t)\right)_N. \end{aligned}$$

Setting $\tau = 1$ leads to

$$\frac{d}{dt}\left(\|v_t\|_{H_a}^2 + \|D_1 v\|_{H_b}^2\right) = -2\left(v_t^T(\alpha v_t - g)\right)_0 - 2\left(v_t^T(\alpha v_t - g)\right)_N. \tag{5}$$

Equation (5) exactly mimics (3), except for the highest frequency mode (see [18]). The problems with the numerical scheme given by (4) are twofold: (1) It does not damp the highest frequency mode (see Figs. 2 and 4), which can be proven with Fourier analysis [18]. (2) For a given order of accuracy, the internal numerical scheme is wider than necessary, leading to lower than optimal numerical accuracy. A remedy would be to employ a narrow-stencil SBP operator for $\partial/\partial x(b\partial/\partial x)$, where $b(x) > 0$.

In [16] we introduced the following definition:

Definition 2.3 Let $D_2^{(b)} = H^{-1}(-M^{(b)} + \bar{B}S)$ approximate $\partial/\partial x(b\partial/\partial x)$, where $b(x) > 0$, using a pth-order accurate narrow-stencil. $D_2^{(b)}$ is said to be a pth-order accurate narrow-diagonal second-derivative SBP operator, if H is diagonal and positive definite, $M^{(b)}$ is symmetric and positive semi-definite, S approximates the first-derivative operator at the boundaries and $\bar{B} = \mathrm{diag}(-b_0, 0, \ldots, 0, b_N)$.

By employing a narrow-diagonal SBP operator $D_2^{(b)}$ in (2), we obtain the semi-discrete approximation

$$\begin{aligned} Av_{tt} = {} & D_2^{(b)} v - H^{-1}\tau e_0\{(\alpha v_t - BSv)_0 - g\} \\ & - H^{-1}\tau e_N\{(\alpha v_t + BSv)_N - g\}. \end{aligned} \tag{6}$$

Applying the energy method by multiplying (6) by $v_t^T H$, adding the transpose and setting $\tau = 1$ lead to

$$\frac{d}{dt}\left(\|v_t\|_{H_a}^2 + v^T M^{(b)} v\right) = -2\left(v_t^T(\alpha v_t - g)\right)_0 - 2\left(v_t^T(\alpha v_t - g)\right)_N. \tag{7}$$

Equation (7) is a semi-discrete analogue to (3), also for the highest frequency mode.

The advantages of employing narrow-diagonal second-derivative SBP operators are that they damp the highest frequency mode, and yield a more accurate representation of $\partial/\partial x(b\partial/\partial x)$. However, such operators have not yet been presented in literature, except for second-order accuracy [16]. In [11] the variable coefficient problem (for the second, fourth and sixth-order case) was analyzed without inclusion of boundaries (i.e., not SBP) and mixed second-derivative terms.

Remark To obtain energy estimates for schemes utilizing both D_1 and $D_2^{(b)}$ requires that both are based on the same norm H.

Remark The boundary closure for a pth-order accurate narrow-diagonal SBP operator is of order $p/2$ (see [17]). The convergence rate for narrow-stencil approximations of second-order hyperbolic problems drops to $(p/2+2)$th-order. (See [8, 27] for more information on the accuracy of finite difference approximations.)

It was shown in [19] that the present Definition 2.3 of a narrow-diagonal second-derivative SBP operators alone does not guarantee stability for problems with a combination of mixed $(\partial^2/\partial x\partial y)$ and non-mixed $(\partial^2/\partial x^2, \partial^2/\partial y^2)$ second-derivatives, such as the

compressible Navier-Stokes equations [19] and the elastic wave equation [1]. In [19] we introduced an important relationship between the existing narrow-diagonal first- and second-derivative (first derived in [17]) SBP operators, referred to as *compatibility*. The main result of that study was to show that compatibility is required to prove stability for problems with a combination of mixed and non-mixed second-derivatives. That study focused on the constant coefficient problems since high-order accurate compatible second-derivative SBP operators with variable coefficients at the time did not exist.

2.2 Compatible Second-Derivative SBP Operators

The main goal of the present study is to derive and construct high-order accurate compatible narrow-diagonal SBP operators for second-derivatives with variable coefficients. The following definition is central in this paper:

Definition 2.4 Let D_1 and $D_2^{(b)}$ be pth-order accurate narrow-diagonal first- and second-derivative SBP operators. If $M^{(b)} = D_1^T H B D_1 + R^{(b)}$, and the remainder $R^{(b)}$ is positive semi-definite, D_1 and $D_2^{(b)}$ are called compatible.

The study of the constant coefficient problem in [19] leads to the following ansatz for the remainders $R^{(b)}$ in the corresponding variable coefficient case, for the second, fourth, sixth and eighth-order cases (starting with the second-order case and ending with the eighth-order case below):

$$
\begin{aligned}
R^{(b)} &= \frac{h^3}{4}(D_2^{(2)})^T C_2^{(2)} B_2^{(2)} D_2^{(2)} \\
R^{(b)} &= \frac{h^5}{18}(D_3^{(4)})^T C_3^{(4)} B_3^{(4)} D_3^{(4)} + \frac{h^7}{144}(D_4^{(4)})^T C_4^{(4)} B_4^{(4)} D_4^{(4)} \\
R^{(b)} &= \frac{h^7}{80}(D_4^{(6)})^T C_4^{(6)} B_4^{(6)} D_4^{(6)} + \frac{h^9}{600}(D_5^{(6)})^T C_5^{(6)} B_5^{(6)} D_5^{(6)} \\
&\quad + \frac{h^{11}}{3600}(D_6^{(6)})^T C_6^{(6)} B_6^{(6)} D_6^{(6)} \\
R^{(b)} &= \frac{h^9}{350}(D_5^{(8)})^T C_5^{(8)} B_5^{(8)} D_5^{(8)} + \frac{h^{11}}{2520}(D_6^{(8)})^T C_6^{(8)} B_6^{(8)} D_6^{(8)} \\
&\quad + \frac{h^{13}}{14700}(D_7^{(8)})^T C_7^{(8)} B_7^{(8)} D_7^{(8)} + \frac{h^{15}}{78400}(D_8^{(8)})^T C_8^{(8)} B_8^{(8)} D_8^{(8)}.
\end{aligned}
\tag{8}
$$

The internal schemes in $D_i^{(p)}$ ($p = 2, 4, 6, 8$, denoting different order of accuracy) are narrow-stencil approximations of $\frac{d^i}{dx^i}$ and $C_i^{(p)}$ are diagonal matrices with non-negative entries, $i = 2, \ldots, 8$. Note that $D_i^{(p)}$ for different orders of accuracy p differ only at the boundaries for a given derivative order (denoted by i). To obtain a narrow stencil operator also for the variable coefficient case, the diagonal and positive matrices $B_i^{(p)}$ have special weights (as listed in the Appendix). This construction guarantees that the $R^{(b)}$ are symmetric and positive semidefinite by construction, up to eighth-order.

The interior scheme is given, since we require minimal width and pth-order accuracy. Left to find are the boundary modifications in $D_i^{(p)}$ and $C_i^{(p)}$ such that the following constraints are met:

1. $D_2^{(b)}$, when $b(x) = 1$, is identical to the compatible constant coefficient second-derivative SBP operators first derived in [17].

2. $C_i^{(p)}$ has non-negative entries.
3. $D_i^{(p)}$ is a consistent approximation of $\frac{d^i}{dx^i}$ at the boundaries.
4. $D_2^{(b)}$ is of order $p/2$ at the boundaries.

Altogether, the above construction leads to large non-linear system of equations, especially for the sixth and eighth-order cases. Typically you need to reduce as much as possible the number of unknowns (in a way that still allows a solution). The first step is to restrict the unknowns in $D_i^{(p)}$ and $C_i^{(p)}$, such that the first three constraints above are met. The most difficult part is to find a valid solution such that the entries in $C_i^{(p)}$ are non-negative. A fruitful approach (found after some testing) is to set as many entries as possible to zero in $C_i^{(p)}$ close to the boundaries and just allow unknowns in a few rows in $D_i^{(p)}$ (typically corresponding to the rows with the unknown entries in $C_i^{(p)}$). Start with as few unknowns as possible (you need at least as many as there are equations). If no solution is found, more unknowns are introduced. If any unknowns are left after fulfilling the first three constraints, they are used to guarantee that the last constraint is met.

After some extensive testing, compatible SBP operators are derived (see Definition 2.4) fulfilling the four constraints above for the second-, fourth- and sixth-order cases, by using the symbolic mathematics software Maple, see Appendix. Strictly speaking the first constraint is not necessary, but it does guarantee that the operators are well behaved, meaning that the spectral radius is small (see, for example, [26]) and that the boundary accuracy is high. In the eighth-order case a solution fulfilling the first constraint could not be found. However, the first constraint is not necessary for stability, but it might influence on efficiency. Also, an earlier observation from the constant coefficient case (not presented here) is that the existing narrow-stencil sixth order discretization is more efficient than the corresponding eighth order. However, the above construction could be useful for other developers since it indicates how to build an eighth order accurate compatible narrow-stencil second derivative SBP operator from an eighth order accurate first derivative SBP operator. We therefore list possible closures in the Appendix also for this case, although no computations have been done in the eighth order case.

3 Efficiency Study in 1-D

The main focus in the present study is to construct compatible narrow-diagonal SBP operators for variable coefficient second derivatives, necessary when proving stability for general multi-D problems involving variable coefficient mixed and non-mixed second-derivatives. The necessary stability constraints (see Definition 2.4) can only be seen in a multi-D setting, proven in Theorem 4.2. The main difference between the narrow-stencil and the corresponding wide-stencil approximation (i.e., when employing only the first derivative SBP operator) lies in the treatment of the pure second-derivative terms (such as $(\mathbf{C}_{11}\mathbf{u}_x)_x$ and $(\mathbf{C}_{22}\mathbf{u}_y)_y$ in (19)). Hence, to motivate the use for narrow-diagonal SBP operators it is enough to compare the accuracy- and stability-properties of the corresponding wide-stencil approximation in a 1-D setting.

The convergence rate is calculated as

$$q = \log_{10}\left(\frac{\|u - v^{(N_1)}\|_h}{\|u - v^{(N_2)}\|_h}\right) \Big/ \log_{10}\left(\frac{N_1}{N_2}\right)^{1/d}, \tag{9}$$

where d is the dimension ($d = 1$ in the 1-D case), u is the analytic solution, and $v^{(N_1)}$ the corresponding numerical solution with N_1 unknowns. $\|u - v^{(N_1)}\|_h$ is the discrete l_2 norm of the error.

We study the 1-D wave equation (2) extended to the spatial domain $-1 \le x \le 1$, where the coefficients $a(x), b(x) > 0$ are discontinuous at $x = 0$, leading to the following problem

$$\begin{aligned} a^{(1)}u_{tt}^{(1)} &= (b^{(1)}u_x^{(1)})_x, \quad -1 \le x \le 0 \\ a^{(2)}u_{tt}^{(2)} &= (b^{(2)}u_x^{(2)})_x, \quad 0 \le x \le 1 \end{aligned}, \tag{10}$$

where $a^{(1)} \neq a^{(2)}$, $b^{(1)} \neq b^{(2)}$. Here $u^{(1,2)}$ denote the solutions corresponding to the left and right domains respectively. We introduce the following coordinate transformations,

$$\begin{aligned} x = x(\xi) &= \xi \left(\frac{e^{-(\xi+\frac{4}{5})^2}}{e^{-(-1+\frac{4}{5})^2}} \right)^l, \quad \xi = [-1, 0], \\ x = x(\xi) &= \xi \left(\frac{e^{-(\xi-\frac{4}{5})^2}}{e^{-(1-\frac{4}{5})^2}} \right)^l, \quad \xi = [0, 1], \end{aligned} \tag{11}$$

in the left and right domains, respectively. Here l is a non-negative integer, where the case $l = 0$ corresponds to the Cartesian case. A larger value on l leads to a denser clustering of grid-points close to the interface and the outer boundaries. The problem (10) transforms to

$$\begin{aligned} \tilde{a}^{(1)}u_{tt}^{(1)} &= (c^{(1)}u_\xi^{(1)})_\xi, \quad -1 \le \xi \le 0 \\ \tilde{a}^{(2)}u_{tt}^{(2)} &= (c^{(2)}u_\xi^{(2)})_\xi, \quad 0 \le \xi \le 1 \end{aligned}, \tag{12}$$

in curvilinear coordinates, where $\tilde{a}^{(1,2)} = a^{(1,2)}x_\xi^{(1,2)}$ and $c^{(1,2)} = b^{(1,2)}/x_\xi^{(1,2)}$. Continuity at the interface ($\xi = 0$) means that the following interface (jump) conditions:

$$u^{(1)} = u^{(2)}, \qquad c^{(1)}u_\xi^{(1)} = c^{(2)}u_\xi^{(2)}, \tag{13}$$

have to be fulfilled. The SAT method of handling discontinuous media is used. To make the paper self contained we write out in detail the SBP-SAT treatment of the 1-D model problem. (A detailed analysis of this particular problem is described in [16].) The semi-discrete approximation of (13) can be written

$$I_1 \equiv v_N^{(1)} - v_0^{(2)} = 0, \qquad I_2 \equiv (\bar{C}^{(1)}Sv^{(1)})_N + (\bar{C}^{(2)}Sv^{(2)})_0 = 0. \tag{14}$$

Here $v^{(1,2)}$ are the solution vectors corresponding to the left and right domains respectively. The left and right domains are discretized using $(N + 1)$ grid points.

A semi-discretization of the Neumann boundary conditions (that are applied at the outer boundaries) are given by

$$L_1^T v^{(1)} = (\bar{C}^{(1)}Sv^{(1)})_0 = g, \qquad L_2^T v^{(2)} = (\bar{C}^{(1)}Sv^{(2)})_N = g. \tag{15}$$

A semi-discretization of (12) using narrow-diagonal SBP operators and the SAT method to impose the semi-discrete interface conditions (14) and boundary conditions (15), can be written:

Table 1 $\log(l_2\text{-}errors)$ and convergence rates for different grid-stretching l (see (11)) in the first test. Sixth-order accurate narrow-stencil

N	$\log l_2{}^{(l=0)}$	$q^{(l=0)}$	$\log l_2{}^{(l=1)}$	$q^{(l=1)}$	$\log l_2{}^{(l=2)}$	$q^{(l=2)}$
51	−2.29	0.00	−2.94	0.00	−2.64	0.00
101	−4.20	6.43	−4.74	6.07	−4.40	5.92
201	−5.91	5.72	−6.54	6.01	−6.19	5.98
401	−7.58	5.59	−8.30	5.86	−7.92	5.79
801	−9.22	5.46	−10.07	5.90	−9.68	5.84

$$
\begin{aligned}
\tilde{A}_1 v_{tt}^{(1)} &= D_2^{(c^{(1)})} v^{(1)} && \tilde{A}_2 v_{tt}^{(2)} = D_2^{(c^{(2)})} v^{(2)} \\
&\quad + \tau H^{-1} e_N(I_1) && \quad - \tau H^{-1} e_0(I_1) \\
&\quad + \beta (\bar{C}^{(1)} S)^T e_N H^{-1}(I_1) && \quad - \beta (\bar{C}^{(2)} S)^T e_0 H^{-1}(I_1) \\
&\quad + \gamma H^{-1} e_N(I_2) && \quad - \gamma H^{-1} e_0(I_2) \\
&\quad - H^{-1} e_0(L_1^T v^{(1)} - g), && \quad + H^{-1} e_N(L_2^T v^{(2)} - g).
\end{aligned} \tag{16}
$$

The following Lemma was first stated in [16]:

Lemma 3.1 *The scheme* (16) *is strictly stable if* $D_2^{c^{(1,2)}}$ *are narrow-diagonal SBP operators,* $\gamma = -\frac{1}{2}$, $\beta = \frac{1}{2}$ *and* $\tau \leq -\frac{c^{(1)}+c^{(2)}}{4h\alpha}$ *hold.*

The proof can be found in [16], where the value of $\alpha = 0.1878715026$ (in the above lemma) is shown for the sixth order case.

3.1 Accuracy Property

In the first test the accuracy properties of the sixth-order accurate wide- and narrow-stencil approximations are compared, for an analytic standing wave solution given by

$$
\begin{aligned}
u^{(1)} &= \cos(\pi \sqrt{b^{(1)} a^{(1)}} t) \cos(\pi a^{(1)} \xi), \quad \xi = [-1, 0], \\
u^{(2)} &= \cos(\pi \sqrt{b^{(2)} a^{(2)}} t) \cos(\pi a^{(2)} \xi), \quad \xi = [0, 1].
\end{aligned} \tag{17}
$$

The analytic solution is constructed such that $u_\xi \neq 0$ at the interface ($\xi = 0$) by choosing $a^{(1)} = 10 + \frac{1}{2}$, $a^{(2)} = 3 + \frac{1}{2}$, $b^{(1)} = a^{(2)}$ and $b^{(2)} = a^{(1)}$. At the outer boundaries we impose homogeneous Neumann boundary conditions. The numerical approximation is run to $t = 0.7$, using a time step $dt = 10^{-4}$. We us a compact fourth-order accurate time discretization (see [16] for details). The convergence study for the sixth-order accurate narrow- and wide-stencil approximations are presented in Tables 1 and 2 respectively.

The conclusion of this first test is that the narrow-stencil approximation is much more efficient than the corresponding wide-stencil approximation. We should mention that the time-step restrictions of the wide- and narrow-stencil approximations are approximately the same.

3.2 Stability Property

In the second test we focus on the stability properties of the narrow- and wide-stencil approximations. In particular the SAT method of handling the discontinuous media (see [16]

Table 2 $\log(l_2\text{-}errors)$ and convergence rates for different grid-stretching l (see (11)) in the first test. Sixth-order accurate wide-stencil

N	$\log l_2{}^{(l=0)}$	$q^{(l=0)}$	$\log l_2{}^{(l=1)}$	$q^{(l=1)}$	$\log l_2{}^{(l=2)}$	$q^{(l=2)}$
51	−1.25	0.00	−1.75	0.00	−1.69	0.00
101	−2.56	4.41	−3.27	5.15	−3.41	5.80
201	−3.86	4.34	−4.87	5.34	−5.10	5.66
401	−5.30	4.83	−6.30	4.76	−6.59	4.96
801	−6.72	4.71	−7.66	4.52	−7.89	4.31

Table 3 $\log(l_2\text{-}errors)$ and convergence rates for the sixth-order SAT method in the second test, comparing the narrow- and wide-stencil approximations

N	$\log l_2{}^{(narrow)}$	$q^{(narrow)}$	$\log l_2{}^{(wide)}$	$q^{(wide)}$
101	−1.39		−1.07	
201	−2.31	3.12	−1.72	2.17
401	−4.23	6.43	−3.30	5.29
801	−6.14	6.37	−4.68	4.62

for details) interface is compared to the method of differentiating across the discontinuity here referred to as the "Ignoring" method. Again the model-problem is given by (10), where $a^{(1)} = 1$, $a^{(2)} = 2$, $b^{(1)} = 2$ and $b^{(2)} = 8$. We now run a Gaussian initial profile to $t = 10$ (see Fig. 1). The reference solution is recorded using 1601 grid-points in each domain. In Table 3 we compare the narrow- and wide-stencil approximations, treating the media jump with the SAT method, using sixth-order accurate SBP operators and a compact fourth-order time-discretization.

In Table 4 we compare the narrow- and wide-stencil approximations when ignoring the media jump, which leads to first-order accurate approximations (see [10] for a detailed convergence study on this problem). In Fig. 2 we present the numerical solutions at $t = 10$ using 201 grid points, comparing both the wide- and narrow-stencil approximations when ignoring the media jump. The highest frequency mode is clearly visible in the wide-stencil approximation. Compare this with the corresponding result using the sixth-order SAT method (using 201 grid-points) in Fig. 1. In Table 5 we compare the narrow- and wide-stencil approximations when ignoring the media jump for the corresponding second-order case, which is the most widely used finite difference approximation in practical applications.

The conclusion of this last study can be summarized in the following: (1) It is very important to use the SAT method of handling the media jump, (2) the narrow-stencil approximation is much more efficient than the corresponding wide-stencil approximation, and (3) if ignoring the media jump, a second-order finite difference scheme can be more efficient than a corresponding higher-order scheme.

4 The 2-D Problem

To simplify the 2-D analysis we introduce some notation, beginning with the Kronecker product:

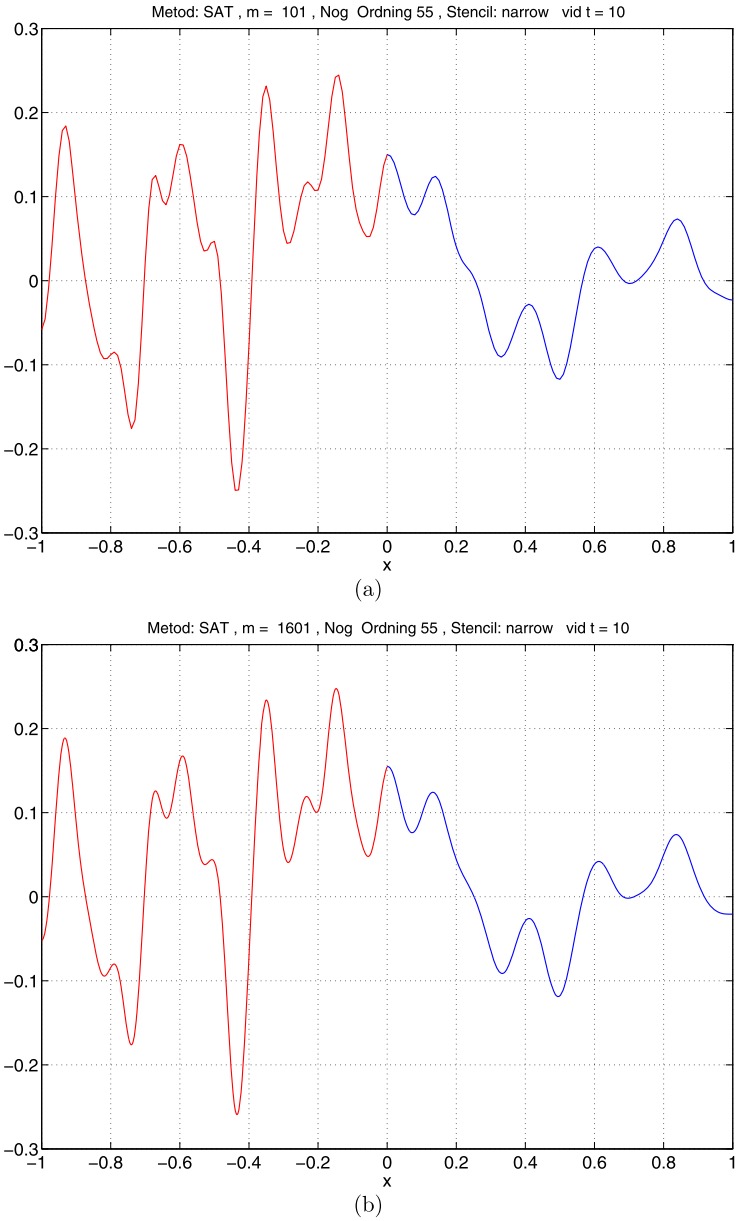

Fig. 1 Solutions at $t = 10$, using the sixth-order accurate narrow-stencil SBP-SAT method, with $N = 201$ (**a**) and $N = 1601$ (**b**), initiated with a Gaussian profile

$$C \otimes D = \begin{bmatrix} c_{0,0}D & \cdots & c_{0,q-1}D \\ \vdots & & \vdots \\ c_{p-1,0}D & \cdots & c_{p-1,q-1}D \end{bmatrix},$$

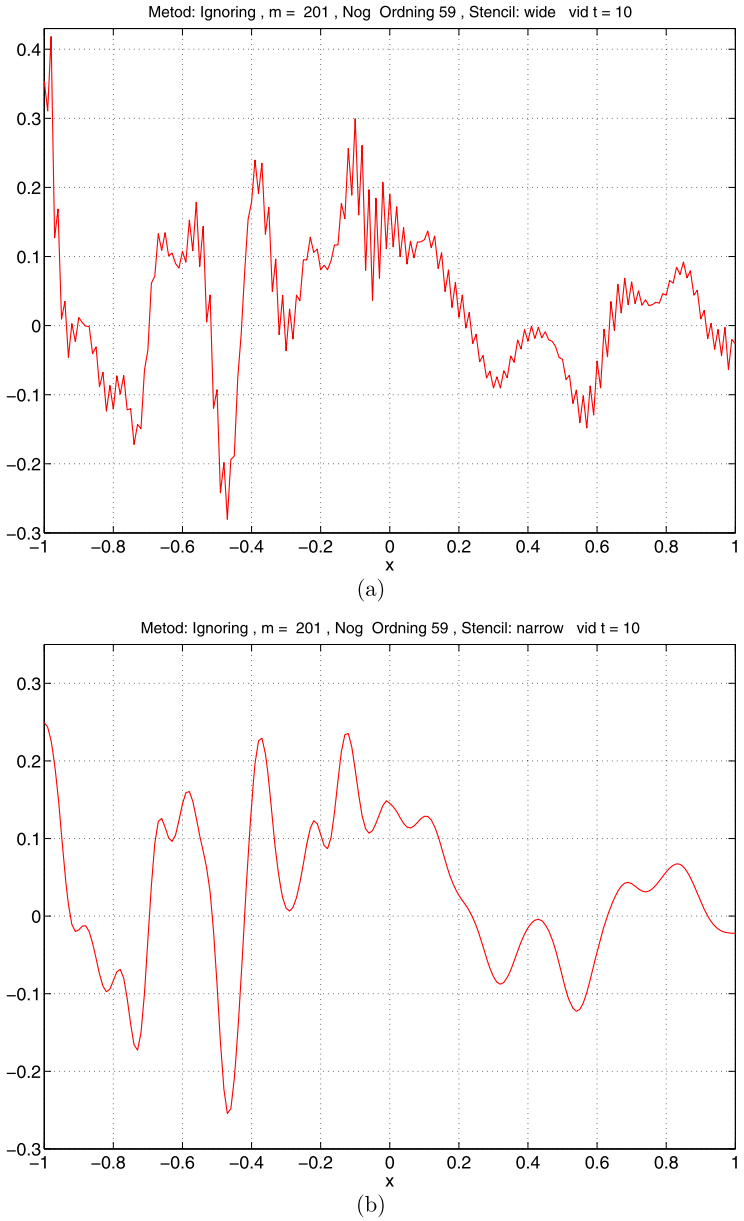

Fig. 2 Solution at $t = 10$ initiated with a Gaussian profile. Comparing the wide-stencil (**a**) and narrow-stencil (**b**) ignoring method using 201 grid-points

where C is a $p \times q$ matrix and D is an $m \times n$ matrix. Two useful rules for the Kronecker product are $(A \otimes B)(C \otimes D) = (AC) \otimes (BD)$ and $(A \otimes B)^T = A^T \otimes B^T$.

The following definition will be used in subsequent sections:

Table 4 $\log(l_2\text{-}errors)$ and convergence rates for the sixth-order Ignoring method in the second test, comparing the narrow- and wide-stencil approximation

N	$\log l_2^{(narrow)}$	$q^{(narrow)}$	$\log l_2^{(wide)}$	$q^{(wide)}$
101	−0.96		−0.94	
201	−1.15	0.64	−1.03	0.28
401	−1.47	1.05	−1.33	1.00
801	−1.78	1.06	−1.66	1.12

Table 5 $\log(l_2\text{-}errors)$ and convergence rates for the second-order SAT and Ignoring method in the second test, using narrow-stencil approximations

N	$\log l_2^{(SAT)}$	$q^{(SAT)}$	$\log l_2^{(Ignoring)}$	$q^{(Ignoring)}$
101	−0.76		−0.94	
201	−0.88	0.40	−0.99	0.18
401	−1.08	0.69	−1.16	0.58
801	−1.64	1.84	−1.67	1.67
1601	−2.23	1.99	−2.15	1.60

Definition 4.1 Let $\bar{x} = (x, y)$ denote grid coordinates in two dimensions. We define the 2-D bounding box $0 \le x \le 1, 0 \le y \le 1$ by $\bar{x} \in \Omega$, and the line $x = 1, 0 \le y \le 1$ by $\bar{x} \in \Omega_{East}$.

The domain Ω is discretized with an $(N+1) \times (M+1)$-point equidistant grid defined as

$$\begin{aligned} x_i &= 0 + ih_x, \quad i = 0, 1, \ldots, N,\ h_x = \tfrac{1}{N}, \\ y_j &= 0 + jh_y, \quad j = 0, 1, \ldots, M,\ h_y = \tfrac{1}{M}. \end{aligned}$$

To simplify notation (without any restriction) we assume the same dimension (N) in both the x- and y-direction. In the following k denotes the number of unknowns in the underlying continuous PDE. The numerical approximation at grid point $(x_i, y_j) \equiv \bar{x}_{i,j}$ is a $1 \times k$-vector denoted $v_{i,j}$. The tensor product derivations are more transparent if we redefine the component vector $v_{i,j}$ as a "vector of vectors." Specifically, define a discrete solution vector $v^T = [v^0, v^1, \ldots, v^N]$, where $v^p = [v_{p,0}, v_{p,1}, \ldots, v_{p,N}]$ is the solution vector at x_p along the y-direction, see Fig. 3. To distinguish whether a 2-D difference operator P is operating in the x- or the y-direction, we use the notations P_x and P_y, respectively. The following 2-D operators are frequently used:

$$\begin{aligned} D_x &= I_k \otimes D_1 \otimes I_N, & D_y &= I_k \otimes I_N \otimes D_1, \\ D_{2x}^{(b)} &= I_k \otimes D_2^{(b)} \otimes I_N, & D_{2y}^{(b)} &= I_k \otimes I_N \otimes D_2^{(b)}, \\ R_x^{(b)} &= I_k \otimes R^{(b)} \otimes I_N, & R_y^{(b)} &= I_k \otimes I_N \otimes R^{(b)}, \\ S_x &= I_k \otimes S \otimes I_N, & S_y &= I_k \otimes I_N \otimes S, \\ B_x &= I_k \otimes B \otimes I_N, & B_y &= I_k \otimes I_N \otimes B, \\ \bar{B}_x &= I_k \otimes \bar{B} \otimes I_N, & \bar{B}_y &= I_k \otimes I_N \otimes \bar{B}, \end{aligned} \tag{18}$$

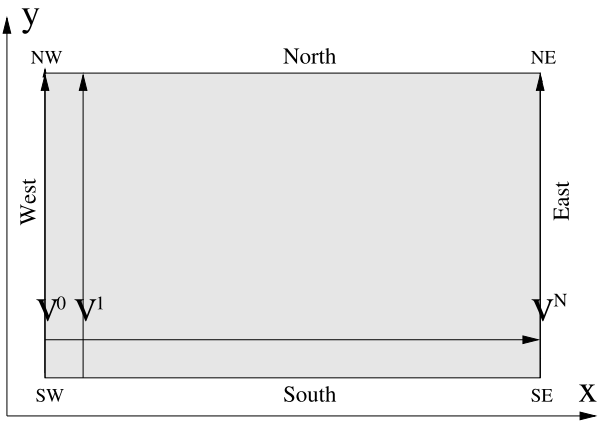

Fig. 3 Domain 2-D

$$H_x = I_k \otimes H \otimes I_N, \qquad H_y = I_k \otimes I_N \otimes H,$$
$$e_{West} = I_k \otimes e_0 \otimes I_N, \qquad e_{South} = I_k \otimes I_N \otimes e_0,$$
$$e_{East} = I_k \otimes e_N \otimes I_N, \qquad e_{North} = I_k \otimes I_N \otimes e_N,$$

where D_1, $D_2^{(B)}$, S, R, B, $\bar{B}$ and H are the 1-D operators introduced in Sect. 2. Note that $D_{2x}^{(b)} = H_x^{-1}(-D_x^T B_x H_x D_x - R_x^{(b)} + \bar{B}_x S_x)$, $D_{2y}^{(b)} = H_y^{-1}(-D_y^T B_y H_y D_y - R_y^{(b)} + \bar{B}_y S_y)$. I_N and I_k are identity matrices of appropriate sizes, and e_0 and e_N are 1-D "boundary" vectors defined by (1). We further introduce the 2-D norm operators $\tilde{H} = H_x H_y$, $\hat{H} = \mathrm{diag}(\tilde{H}, \tilde{H})$.

4.1 Analysis

Our main focus in the present study is on deriving narrow-stencil high-order accurate compatible second-derivative SBP operators with variable coefficients. These operators are necessary in order to derive strictly stable narrow-stencil approximations for problems with a combination of mixed $\partial/\partial x(b_{12}(x,y)\partial/\partial y)$, $\partial/\partial y(b_{21}(x,y)\partial/\partial x)$ and pure $\partial/\partial x(b_{11}(x,y)\partial/\partial x)$, $\partial/\partial y(b_{22}(x,y)\partial/\partial y)$ second-derivatives with variable coefficients, such as the compressible Navier-Stokes equations and various second-order hyperbolic systems on curvilinear grids. A narrow-stencil approximation will efficiently damp the highest frequency mode (as we saw in the previous section). In Fig. 4 we compare the sixth-order accurate narrow-stencil approximation to the wide-stencil approximation of the second order wave equation on a curvilinear 2-D grid (that can formally be written as (19) with $k = 1$). The simulation is initiated with a rather sharp Gaussian profile and run to $t = 10$. At the outer boundaries we set homogeneous Neumann boundary conditions. The highest frequency mode is clearly visible in the wide-stencil approximation.

Consider the 2-D hyperbolic system (with k unknowns):

$$\mathbf{A}\mathbf{u}_{tt} = \left(\mathbf{C}_{11}\mathbf{u}_x + \mathbf{C}_{12}\mathbf{u}_y\right)_x + \left(\mathbf{C}_{21}\mathbf{u}_x + \mathbf{C}_{22}\mathbf{u}_y\right)_y, \quad \bar{x} \in \Omega. \tag{19}$$

We Introduce

$$\mathbf{C} = \begin{bmatrix} \mathbf{C}_{11} & \mathbf{C}_{12} \\ \mathbf{C}_{21} & \mathbf{C}_{22} \end{bmatrix}, \qquad \hat{\mathbf{u}} = \begin{bmatrix} \mathbf{u}_x \\ \mathbf{u}_y \end{bmatrix},$$

and require the $2k \times 2k$ matrix $\mathbf{C}$ to be symmetric and positive semidefinite. The discrete counterpart to $\hat{\mathbf{u}}$ is given by

$$\hat{v} = \begin{bmatrix} D_x v \\ D_y v \end{bmatrix}.$$

We consider the following boundary conditions at the 4 boundaries (East, West, North, South):

$$\begin{aligned} &\Phi_{East}\mathbf{u}_t + \mathbf{C}_{11}\mathbf{u}_x + \mathbf{C}_{12}\mathbf{u}_y = \mathbf{g}, \quad \bar{x} \in \Omega_{East}, \\ &\Phi_{West}\mathbf{u}_t - \mathbf{C}_{11}\mathbf{u}_x - \mathbf{C}_{12}\mathbf{u}_y = \mathbf{g}, \quad \bar{x} \in \Omega_{West}, \\ &\Phi_{North}\mathbf{u}_t + \mathbf{C}_{21}\mathbf{u}_x + \mathbf{C}_{22}\mathbf{u}_y = \mathbf{g}, \quad \bar{x} \in \Omega_{North}, \\ &\Phi_{South}\mathbf{u}_t - \mathbf{C}_{21}\mathbf{u}_x - \mathbf{C}_{22}\mathbf{u}_y = \mathbf{g}, \quad \bar{x} \in \Omega_{South}. \end{aligned} \tag{20}$$

Remark Other type of well-posed boundary conditions, like Dirichlet can also be used. However, the main focus in this paper is on the derivation of compatible second-derivative SBP operators.

Multiplying (19) by $\mathbf{u}_t$, and integrating by parts with the use of (20) lead to

$$E_t = BT_{East} + BT_{West} + BT_{North} + BT_{South}, \tag{21}$$

where

$$E = \int\int_{\Omega} \mathbf{u}_t^T \mathbf{A}\mathbf{u}_t + \hat{\mathbf{u}}^T \mathbf{C}\hat{\mathbf{u}}\, dxdy, \tag{22}$$

and

$$\begin{aligned} BT_{East} &= -2\textstyle\int_{\partial\Omega_{East}} \mathbf{u}_t^T \left(\mathbf{\Phi}_{East}\mathbf{u}_t - \mathbf{g}\right) dy, \\ BT_{West} &= -2\textstyle\int_{\partial\Omega_{West}} \mathbf{u}_t^T \left(\mathbf{\Phi}_{West}\mathbf{u}_t - \mathbf{g}\right) dy, \\ BT_{North} &= -2\textstyle\int_{\partial\Omega_{North}} \mathbf{u}_t^T \left(\mathbf{\Phi}_{North}\mathbf{u}_t - \mathbf{g}\right) dx, \\ BT_{South} &= -2\textstyle\int_{\partial\Omega_{South}} \mathbf{u}_t^T \left(\mathbf{\Phi}_{South}\mathbf{u}_t - \mathbf{g}\right) dx. \end{aligned} \tag{23}$$

An energy estimate exists if $\mathbf{\Phi}_{East,\,West,\,North,\,South}$ are positive semidefinite.

A corresponding semi-discrete approximation of (19) with the boundary conditions (20) can be written

$$Av_{tt} = D_x\left(C_{11}D_x v + C_{12}D_y v\right) + D_y\left(C_{21}D_x v + C_{22}D_y v\right) + SAT_{E,W,N,S}, \tag{24}$$

where $SAT_{E,W,N,S}$ imposes the boundary conditions (20) using the penalty technique

$$\begin{aligned} SAT_E &= -H_x^{-1} e_{East}\left((\Phi_{East}v_t + C_{11}D_x v + C_{12}D_y v)_E - g\right), \\ SAT_W &= -H_x^{-1} e_{West}\left((\Phi_{West}v_t - C_{11}D_x v - C_{12}D_y v)_W - g\right), \\ SAT_N &= -H_y^{-1} e_{North}\left((\Phi_{North}v_t + C_{21}D_x v + C_{22}D_y v)_N - g\right), \\ SAT_S &= -H_y^{-1} e_{South}\left((\Phi_{South}v_t - C_{21}D_x v - C_{22}D_y v)_S - g\right). \end{aligned}$$

In the following, the subscripts E, W, N, S indicates that the quantities reside on the East, West, North and South boundaries (see Fig. 3).

Apply the energy method by multiplying (24) by $v_t^T \tilde{H}$, and adding the transpose, leading to (21), where now

$$E = v_t^T A \tilde{H} v_t + \hat{v}^T C \hat{H} \hat{v}, \tag{25}$$

and

$$\begin{aligned} BT_{East} &= -2\left(v_t^T H_y \left(\Phi_{East} v_t - g\right)\right)_E, \\ BT_{West} &= -2\left(v_t^T H_y \left(\Phi_{West} v_t - g\right)\right)_W, \\ BT_{North} &= -2\left(v_t^T H_x \left(\Phi_{North} v_t - g\right)\right)_N, \\ BT_{South} &= -2\left(v_t^T H_x \left(\Phi_{South} v_t - g\right)\right)_S. \end{aligned} \tag{26}$$

Hence, the semi-discrete energy estimate exactly mimics the continuous energy estimate, except for the highest frequency mode (see Fig. 4). This can potentially alter the scheme unstable. The reason for this is that the first derivative SBP operator used to build the energy term $\hat{v}^T C \hat{H} \hat{v}$ in (25) does not damp spurious oscillations (i.e., the highest frequency mode).

Remark The compatible narrow-stencil second-derivative SBP operators are constructed to mimic the continuous energy estimate for problems such as (19), and introduce a mechanism for damping the highest frequency mode.

A semidiscretization of (19) using compatible narrow-diagonal SBP operators and the SAT method can be written as

$$A v_{tt} = D_{2x}^{(C_{11})} v + D_x C_{12} D_y v + D_y C_{21} D_x v + D_{2y}^{(C_{22})} v + S\tilde{A}T_{E,W,N,S}, \tag{27}$$

where $S\tilde{A}T_{E,W,N,S}$ are given by

$$\begin{aligned} S\tilde{A}T_E &= -H_x^{-1} e_{East} \left((\Phi_{East} v_t + C_{11} S_x v + C_{12} D_y v)_E - g \right), \\ S\tilde{A}T_W &= -H_x^{-1} e_{West} \left((\Phi_{West} v_t - C_{11} S_x v - C_{12} D_y v)_W - g \right), \\ S\tilde{A}T_N &= -H_y^{-1} e_{North} \left((\Phi_{North} v_t + C_{21} D_x v + C_{22} S_y v)_N - g \right), \\ S\tilde{A}T_S &= -H_y^{-1} e_{South} \left((\Phi_{South} v_t - C_{21} D_x v - C_{22} S_y v)_S - g \right). \end{aligned}$$

(The differences between (24) and (27) are that we have replaced $D_x C_{11} D_x$, and $D_y C_{22} D_y$ with $D_{2x}^{(C_{11})}$ and $D_{2y}^{(C_{22})}$ respectively, and that we have replaced D_x and D_y with S_x and S_y at the appropriate places in the penalty terms.)

One of the main results of this paper is stated in the following theorem:

Theorem 4.2 *The scheme (27) is strictly stable if D_1, $D_2^{(C_{22})}$ and $D_2^{(C_{11})}$ are compatible narrow-diagonal first- and second-derivative SBP operators and $\Phi_{East,West,North,South}$ are positive semidefinite.*

Proof Multiplying (27) by $v_t^T \tilde{H}$ from the left and adding the transpose lead to

$$E_t = BT_{East} + BT_{West} + BT_{North} + BT_{South},$$

where

$$E = v_t^T A \tilde{H} v_t + \hat{v}^T C \hat{H} \hat{v} + v^T H_y R_x^{(C_{11})} v + v^T H_x R_y^{(C_{22})} v,$$

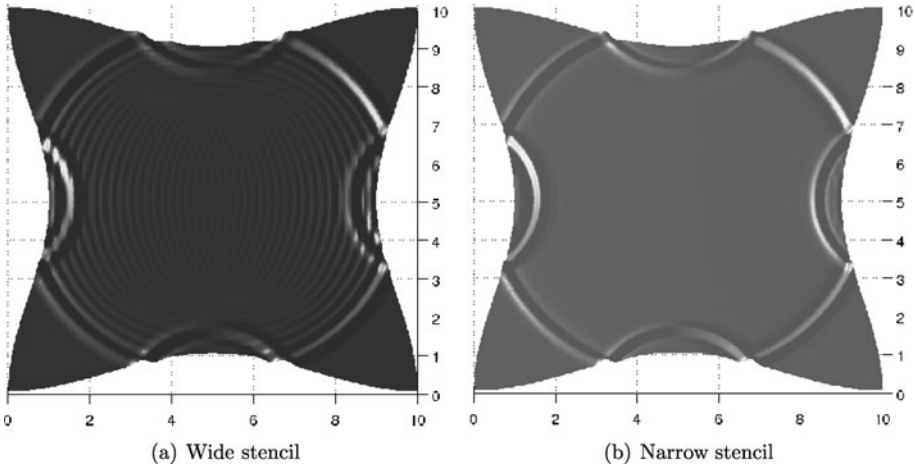

Fig. 4 Comparing the sixth-order accurate wide-stencil (**a**) and narrow-stencil (**b**) approximations of the second order wave equation on a curvilinear 2-D grid. Initiated with a Gaussian profile. The π-mode is clearly visible in (**a**)

and

$$
\begin{aligned}
BT_{East} &= -2\left(v_t^T H_y \left(\Phi_{East} v_t - g\right)\right)_E, \\
BT_{West} &= -2\left(v_t^T H_y \left(\Phi_{West} v_t - g\right)\right)_W, \\
BT_{North} &= -2\left(v_t^T H_x \left(\Phi_{North} v_t - g\right)\right)_N, \\
BT_{South} &= -2\left(v_t^T H_x \left(\Phi_{South} v_t - g\right)\right)_S.
\end{aligned}
$$

The semi-discrete energy estimate exactly mimics the continuous energy estimate if and only if $R_x^{(C_{11})}$ and $R_y^{(C_{22})}$ are positive semi-definite. Since D_1, $D_2^{(C_{22})}$ and $D_2^{(C_{11})}$ are compatible, stability follows if $\Phi_{East,West,North,South}$ are positive semidefinite. □

Remark The additional (small) energy terms $v^T H_y R_x^{(C_{11})} v$ and $v^T H_x R_y^{(C_{22})} v$ in Theorem 4.2 introduce a mechanism for efficient damping of spurious oscillations (see Fig. 4), without destroying accuracy and the energy estimate.

Remark Theorem 4.2 shows why it is necessary to employ compatible narrow-diagonal SBP operators (see Definition 2.4) to exactly mimic the continuous energy estimate for multi-D problems consisting of mixed and pure second-derivative terms, and hence proving strict stability.

5 Conclusions

Our approach has been to construct narrow-stencil SBP operators for variable coefficient second-derivatives, with a property referred to as compatibility. Together with the SAT technique to impose boundary and interface conditions, strict stability can be shown using the energy method, for general second-order hyperbolic (and parabolic) problems. The main objective was to construct SBP operators that combined the following desirable properties:

- stability by construction in combination with the existing first derivative SBP operators,
- capable of maintaining the overall convergence rate,
- capable of maintaining simplicity of the numerical scheme.

To achieve the three properties above, we have constructed SBP operators with the following requirements: (1) We mimic the continuous energy estimate for general second-order 2-D problems (the extension to 3-D is straightforward) by requiring compatibility with the first derivative SBP operators. (2) They have the same order of accuracy as the corresponding wide-stencil approximation. (3) They are of minimal width in the interior.

Numerical computations in 1-D corroborate the stability- and accuracy-properties and also show that narrow-stencil approximations are more accurate and robust than the corresponding wide stencil approximations.

Appendix A: Operators

Here we present the compatible second-, fourth- sixth- and eighth-order accurate narrow-diagonal SBP operators, defined in Sect. 2.2. The first-derivative SBP operators are given by $H^{-1}Q$, where Q can be found in [17]. The second-derivative operator, $D_2^{(b)} = H^{-1}(-M^{(b)} + \bar{B}S)$, approximate $\partial/\partial x(b\partial/\partial x)$, where $b(x) > 0$, using a pth-order accurate narrow-stencil. $M^{(b)}$ is symmetric and positive semi-definite, S approximates the first-derivative operator at the boundaries and $\bar{B} = \mathrm{diag}(-b_0, 0 \ldots, 0, b_N)$.

In Sect. 2.2 we showed that if $M^{(b)} = D_1^T H B D_1 + R^{(b)}$, and the remainder $R^{(b)}$ is positive semi-definite, D_1 and $D_2^{(b)}$ are called *compatible*. The remaining terms are defined in (8).

A.1 Second-Order Accurate

For the second-order case we have

$$S = \frac{1}{h}\begin{bmatrix} -\frac{3}{2} & 2 & -\frac{1}{2} & & \\ & 1 & & & \\ & & \ddots & & \\ & & & 1 & \\ & & \frac{1}{2} & -2 & \frac{3}{2} \end{bmatrix}, \qquad H = \frac{h}{2}\begin{bmatrix} 1 & & & & \\ & 2 & & & \\ & & \ddots & & \\ & & & 2 & \\ & & & & 1 \end{bmatrix}.$$

The operators $D_2^{(2)}$ and $C_2^{(2)}$ are given by:

$$D_2^{(2)} = \begin{bmatrix} 1 & -2 & 1 & & & \\ 1 & -2 & 1 & & & \\ & 1 & -2 & 1 & & \\ & & \ddots & \ddots & \ddots & \\ & & 1 & -2 & 1 & \\ & & & 1 & -2 & 1 \\ & & & 1 & -2 & 1 \end{bmatrix}, \qquad C_2^{(2)} = \begin{bmatrix} 0 & & & & \\ & 1 & & & \\ & & \ddots & & \\ & & & 1 & \\ & & & & 0 \end{bmatrix}.$$

The $B_2^{(2)}$ matrix is given by $(B_2^{(2)})_{i,i} = b_i$.

The left boundary closure of $M^{(b)}$ (given by a 3×3 matrix) is given by

$$\begin{bmatrix} \frac{1}{2}b_1 + \frac{1}{2}b_2 & -\frac{1}{2}b_1 - \frac{1}{2}b_2 & 0 \\ -\frac{1}{2}b_1 - \frac{1}{2}b_2 & \frac{1}{2}b_1 + b_2 + \frac{1}{2}b_3 & -\frac{1}{2}b_2 - \frac{1}{2}b_3 \\ 0 & -\frac{1}{2}b_2 - \frac{1}{2}b_3 & \frac{1}{2}b_2 + b_3 + \frac{1}{2}b_4 \end{bmatrix}.$$

The corresponding right boundary closure is given by replacing $b_i \rightarrow b_{N+1-i}$ for $i = 1..4$ followed by a permutation of both rows and columns.

The interior stencil of $M^{(b)}$ at row i is given by ($i = 4 \ldots N-3$):

$$\begin{aligned} m_{i,i-1} &= -\frac{1}{2}b_{i-1} - \frac{1}{2}b_i \\ m_{i,i} &= \frac{1}{2}b_{i-1} + b_i + \frac{1}{2}b_{i+1} \\ m_{i,i+1} &= -\frac{1}{2}b_i - \frac{1}{2}b_{i+1}. \end{aligned}$$

A.2 Fourth-Order Accurate

The third-order accurate boundary derivative operator S is given by,

$$S = \frac{1}{h}\begin{bmatrix} -\frac{11}{6} & 3 & -\frac{3}{2} & \frac{1}{3} & & & \\ & 0 & & & & & \\ & & & \ddots & & & \\ & & & & & 0 & \\ & & & & & & \\ & & & -\frac{1}{3} & \frac{3}{2} & -3 & \frac{11}{6} \end{bmatrix}.$$

The discrete norm H is given by

$$H = h\begin{bmatrix} \frac{17}{48} & & & & & & \\ & \frac{59}{48} & & & & & \\ & & \frac{43}{48} & & & & \\ & & & \frac{49}{48} & & & \\ & & & & 1 & & \\ & & & & & \ddots & \end{bmatrix}.$$

The difference operator $D_3^{(4)}$:

$$\begin{bmatrix} -1 & 3 & -3 & 1 & & & & & & & \\ -1 & 3 & -3 & 1 & & & & & & & \\ d3_1 & d3_2 & d3_3 & d3_4 & d3_5 & d3_6 & & & & & \\ & & -1 & 3 & -3 & 1 & & & & & \\ & & & \ddots & \ddots & \ddots & \ddots & & & & \\ & & & & & -1 & 3 & -3 & 1 & & \\ & & & & -d3_6 & -d3_5 & -d3_4 & -d3_3 & -d3_2 & -d3_1 & \\ & & & & & & -1 & 3 & -3 & 1 & \\ & & & & & & -1 & 3 & -3 & 1 & \end{bmatrix},$$

where

$$d3_1 = -\frac{185893}{301051}, \qquad d3_4 = -\frac{36887526683}{54642863857},$$
$$d3_2 = \frac{79000249461}{54642863857}, \qquad d3_5 = \frac{26183621850}{54642863857},$$
$$d3_3 = -\frac{33235054191}{54642863857}, \qquad d4_6 = -\frac{4386}{181507}.$$

The difference operator $D_4^{(4)}$:

$$\begin{bmatrix}
1 & -4 & 6 & -4 & 1 & & & & & \\
1 & -4 & 6 & -4 & 1 & & & & & \\
1 & -4 & 6 & -4 & 1 & & & & & \\
 & 1 & -4 & 6 & -4 & 1 & & & & \\
 & & \ddots & \ddots & \ddots & \ddots & \ddots & & & \\
 & & & & 1 & -4 & 6 & -4 & 1 & \\
 & & & & & 1 & -4 & 6 & -4 & 1 \\
 & & & & & 1 & -4 & 6 & -4 & 1 \\
 & & & & & 1 & -4 & 6 & -4 & 1
\end{bmatrix}.$$

The left boundary closure of the diagonal matrix $C_3^{(4)}$ is given by:

$$\begin{bmatrix} 0 & 0 & \frac{163928591571}{53268010936} & \frac{189284}{185893} & 1 & \cdots \end{bmatrix}.$$

The right boundary closure of the diagonal matrix $C_3^{(4)}$ is given by:

$$\begin{bmatrix} \cdots & 1 & \frac{189284}{185893} & 0 & \frac{163928591571}{53268010936} & 0 & 0 \end{bmatrix}.$$

The left boundary closure of the diagonal matrix $C_4^{(4)}$ is given by:

$$\begin{bmatrix} 0 & 0 & \frac{1644330}{301051} & \frac{156114}{181507} & 1 & \cdots \end{bmatrix}.$$

The corresponding right boundary closure is given by a permutation of both rows and columns.

The $B^{(4)}$ matrices are given by

$$\begin{aligned} (B_3^{(4)})_{i,i} &= \frac{1}{2}(b_i + b_{i+1}) \\ (B_4^{(4)})_{i,i} &= b_i \end{aligned}.$$

The interior stencil of $-M^{(b)}$ at row i is given by ($i = 7 \ldots N-6$):

$$
\begin{aligned}
m_{i,i-2} &= \frac{1}{6}b_{i-1} - \frac{1}{8}b_{i-2} - \frac{1}{8}b_i,\\
m_{i,i-1} &= \frac{1}{6}b_{i-2} + \frac{1}{6}b_{i+1} + \frac{1}{2}b_{i-1} + \frac{1}{2}b_i,\\
m_{i,i} &= -\frac{1}{24}b_{i-2} - \frac{5}{6}b_{i-1} - \frac{5}{6}b_{i+1} - \frac{1}{24}b_{i+2} - \frac{3}{4}b_i,\\
m_{i,i+1} &= \frac{1}{6}b_{i-1} + \frac{1}{6}b_{i+2} + \frac{1}{2}b_i + \frac{1}{2}b_{i+1},\\
m_{i,i+2} &= \frac{1}{6}b_{i+1} - \frac{1}{8}b_i - \frac{1}{8}b_{i+2}.
\end{aligned}
$$

The left boundary closure of $-M^{(b)}$ (given by a 6×6 matrix) is given by

$$
\begin{aligned}
m_{1,1} &= \frac{12}{17}b_1 + \frac{59}{192}b_2 + \frac{27010400129}{345067064608}b_3 + \frac{69462376031}{2070402387648}b_4,\\
m_{1,2} &= -\frac{59}{68}b_1 - \frac{6025413881}{21126554976}b_3 - \frac{537416663}{7042184992}b_4,\\
m_{1,3} &= \frac{2}{17}b_1 - \frac{59}{192}b_2 + \frac{213318005}{16049630912}b_4 + \frac{2083938599}{8024815456}b_3,\\
m_{1,4} &= \frac{3}{68}b_1 - \frac{1244724001}{21126554976}b_3 + \frac{752806667}{21126554976}b_4,\\
m_{1,5} &= \frac{49579087}{10149031312}b_3 - \frac{49579087}{10149031312}b_4,\\
m_{1,6} &= -\frac{1}{784}b_4 + \frac{1}{784}b_3,\\
m_{2,2} &= \frac{3481}{3264}b_1 + \frac{9258282831623875}{7669235228057664}b_3 + \frac{236024329996203}{1278205871342944}b_4,\\
m_{2,3} &= -\frac{59}{408}b_1 - \frac{29294615794607}{29725717938208}b_3 - \frac{2944673881023}{29725717938208}b_4,\\
m_{2,4} &= -\frac{59}{1088}b_1 + \frac{260297319232891}{2556411742685888}b_3 - \frac{60834186813841}{1278205871342944}b_4,\\
m_{2,5} &= -\frac{1328188692663}{37594290333616}b_3 + \frac{1328188692663}{37594290333616}b_4,\\
m_{2,6} &= -\frac{8673}{2904112}b_3 + \frac{8673}{2904112}b_4,\\
m_{3,3} &= \frac{1}{51}b_1 + \frac{59}{192}b_2 + \frac{13777050223300597}{26218083221499456}b_4 + \frac{564461}{13384296}b_5\\
&\quad + \frac{378288882302546512209}{270764341349677687456}b_3,
\end{aligned}
$$

$$m_{3,4} = \frac{1}{136}b_1 - \frac{125059}{743572}b_5 - \frac{4836340090442187227}{5525802884687299744}b_3 - \frac{17220493277981}{89177153814624}b_4,$$

$$m_{3,5} = -\frac{10532412077335}{42840005263888}b_4 + \frac{1613976761032884305}{7963657098519931984}b_3 + \frac{564461}{4461432}b_5,$$

$$m_{3,6} = -\frac{960119}{1280713392}b_4 - \frac{3391}{6692148}b_5 + \frac{33235054191}{26452850508784}b_3,$$

$$m_{4,4} = \frac{3}{1088}b_1 + \frac{507284006600757858213}{4752190480831077779 84}b_3 + \frac{1869103}{2230716}b_5 + \frac{1}{24}b_6 + \frac{1950062198436997}{3834617614028832}b_4,$$

$$m_{4,5} = -\frac{4959271814984644613}{20965546238960637264}b_3 - \frac{1}{6}b_6 - \frac{15998714909649}{37594290333616}b_4 - \frac{375177}{743572}b_5,$$

$$m_{4,6} = -\frac{368395}{2230716}b_5 + \frac{752806667}{539854092016}b_3 + \frac{1063649}{8712336}b_4 + \frac{1}{8}b_6,$$

$$m_{5,5} = \frac{8386761355510099813}{1284139707136339032 42}b_3 + \frac{2224717261773437}{2763180339520776}b_4 + \frac{5}{6}b_6 + \frac{1}{24}b_7 + \frac{280535}{371786}b_5,$$

$$m_{5,6} = -\frac{35039615}{213452232}b_4 - \frac{1}{6}b_7 - \frac{13091810925}{13226425254392}b_3 - \frac{1118749}{2230716}b_5 - \frac{1}{2}b_6,$$

$$m_{6,6} = \frac{3290636}{80044587}b_4 + \frac{5580181}{6692148}b_5 + \frac{5}{6}b_7 + \frac{1}{24}b_8 + \frac{660204843}{13226425254392}b_3 + \frac{3}{4}b_6.$$

The corresponding right boundary closure is given by replacing $b_i \to b_{N+1-i}$ for $i = 1..8$ followed by a permutation of both rows and columns. Let $m_{i,j}$ be the coefficient at row i and column j in $M^{(b)}$. The matrix $M^{(b)}$ is symmetric, which means that it is completely defined by the upper triangular part, i.e., all $m_{i,j}$, $i = 1..N$, $j = i..N$.

A.3 Sixth-Order Accurate

The discrete norm H is defined:

$$H = h\begin{bmatrix} \frac{13649}{43200} & & & & & & & & \\ & \frac{12013}{8640} & & & & & & & \\ & & \frac{2711}{4320} & & & & & & \\ & & & \frac{5359}{4320} & & & & & \\ & & & & \frac{7877}{8640} & & & & \\ & & & & & \frac{43801}{43200} & & & \\ & & & & & & 1 & & \\ & & & & & & & \ddots & \end{bmatrix}.$$

The 5th-order accurate boundary derivative operator is given by:

$$S = \frac{1}{h}\begin{bmatrix} -\frac{25}{12} & 4 & -3 & \frac{4}{3} & \frac{1}{4} & & \\ & & 1 & & & & \\ & & & \ddots & & & \\ & & & & 1 & & \\ & & \frac{1}{4} & -\frac{4}{3} & 3 & -4 & \frac{25}{12} \end{bmatrix}.$$

The difference operator $D_4^{(6)}$:

$$\begin{bmatrix}
1 & -4 & 6 & -4 & 1 & & & & & & & & \\
1 & -4 & 6 & -4 & 1 & & & & & & & & \\
1 & -4 & 6 & -4 & 1 & & & & & & & & \\
 & 1 & -4 & 6 & -4 & 1 & & & & & & & \\
 & & 1 & -4 & 6 & -4 & 1 & & & & & & \\
d4_1 & d4_2 & d4_3 & d4_4 & d4_5 & d4_6 & d4_7 & d4_8 & d4_9 & & & & \\
 & & & & 1 & -4 & 6 & -4 & 1 & & & & \\
 & & & & \ddots & \ddots & \ddots & \ddots & \ddots & & & & \\
 & & & & & 1 & -4 & 6 & -4 & 1 & & & \\
 & & & & & d4_9 & d4_8 & d4_7 & d4_6 & d4_5 & d4_4 & d4_3 & d4_2 & d4_1 \\
 & & & & & & & 1 & -4 & 6 & -4 & 1 & & \\
 & & & & & & & & 1 & -4 & 6 & -4 & 1 & \\
 & & & & & & & & & 1 & -4 & 6 & -4 & 1 \\
 & & & & & & & & & 1 & -4 & 6 & -4 & 1 \\
 & & & & & & & & & 1 & -4 & 6 & -4 & 1
\end{bmatrix},$$

where

$$\begin{aligned}
d4_1 &= 0.43819837221111761389, & d4_6 &= 0.44412187877629861379,\\
d4_2 &= -1.3130959257572520973, & d4_7 &= -0.14810645777705395814,\\
d4_3 &= 0.94797803521609260191, & d4_8 &= 0.068316245634253478727,\\
d4_4 &= 0.62436372993537192414, & d4_9 &= -0.0047580470461699605110.\\
d4_5 &= -1.0570178311926582165,
\end{aligned}$$

The difference operator $D_5^{(6)}$:

$$
\begin{bmatrix}
-1 & 5 & -10 & 10 & -5 & 1 & & & & & \\
-1 & 5 & -10 & 10 & -5 & 1 & & & & & \\
-1 & 5 & -10 & 10 & -5 & 1 & & & & & \\
 & -1 & 5 & -10 & 10 & -5 & 1 & & & & \\
 & & -1 & 5 & -10 & 10 & -5 & 1 & & & \\
d5_1 & d5_2 & d5_3 & d5_4 & d5_5 & d5_6 & d5_7 & d5_8 & d5_9 & & \\
 & & & & -1 & 5 & -10 & 10 & -5 & 1 & \\
 & & & \ddots & \ddots & \ddots & \ddots & \ddots & \ddots & & \\
 & & & -1 & 5 & -10 & 10 & -5 & 1 & & \\
 & & -d5_9 & -d5_8 & -d5_7 & -d5_6 & -d5_5 & -d5_4 & -d5_3 & -d5_2 & -d5_1 \\
 & & & & -1 & 5 & -10 & 10 & -5 & 1 & \\
 & & & & & -1 & 5 & -10 & 10 & -5 & 1 \\
 & & & & & -1 & 5 & -10 & 10 & -5 & 1 \\
 & & & & & -1 & 5 & -10 & 10 & -5 & 1 \\
 & & & & & -1 & 5 & -10 & 10 & -5 & 1
\end{bmatrix},
$$

where

$$
\begin{aligned}
d5_1 &= -0.52131894522031211822, & d5_6 &= 0.99549078638797583937,\\
d5_2 &= 2.2819596734201098934, & d5_7 &= -0.86326027050414424911,\\
d5_3 &= -3.7719045450737321464, & d5_8 &= 0.32111212717600079458,\\
d5_4 &= 2.9041350609575637367, & d5_9 &= -0.027844354179627268409.\\
d5_5 &= -1.3183695329638344819,
\end{aligned}
$$

The difference operator $D_6^{(6)}$:

$$
\begin{bmatrix}
1 & -6 & 15 & -20 & 15 & -6 & 1 & & & & \\
1 & -6 & 15 & -20 & 15 & -6 & 1 & & & & \\
1 & -6 & 15 & -20 & 15 & -6 & 1 & & & & \\
1 & -6 & 15 & -20 & 15 & -6 & 1 & & & & \\
d6_1 & d6_2 & d6_3 & d6_4 & d6_5 & d6_6 & d6_7 & d6_8 & d6_9 & & \\
d6_{11} & d6_{12} & d6_{13} & d6_{14} & d6_{15} & d6_{16} & d6_{17} & d6_{18} & d6_{19} & & \\
 & & & 1 & -6 & 15 & -20 & 15 & -6 & 1 & \\
 & & \ddots & \ddots & \ddots & \ddots & \ddots & \ddots & & & \\
 & 1 & -6 & 15 & -20 & 15 & -6 & 1 & & & \\
 & & d6_{19} & d6_{18} & d6_{17} & d6_{16} & d6_{15} & d6_{14} & d6_{13} & d6_{12} & d6_{11} \\
 & & d6_9 & d6_8 & d6_7 & d6_6 & d6_5 & d6_4 & d6_3 & d6_2 & d6_1 \\
 & & & & 1 & -6 & 15 & -20 & 15 & -6 & 1 \\
 & & & & 1 & -6 & 15 & -20 & 15 & -6 & 1 \\
 & & & & 1 & -6 & 15 & -20 & 15 & -6 & 1 \\
 & & & & 1 & -6 & 15 & -20 & 15 & -6 & 1
\end{bmatrix},
$$

where

$$
\begin{aligned}
d6_1 &= 0.75842303723660880327, & d6_{11} &= 0.13990577549425331936,\\
d6_2 &= -4.2539074383142963409, & d6_{12} &= 0.19188572768373149785,\\
d6_3 &= 9.5415070255750278950, & d6_{13} &= -4.2605618076252134271,\\
d6_4 &= -10.388676034100037193, & d6_{14} &= 13.699047136714733223,\\
d6_5 &= 4.6179225213125232458, & d6_{15} &= -21.096213322723799491,\\
d6_6 &= 1.0, & d6_{16} &= 18.054894179643345962,\\
d6_7 &= -1.8471690085250092983, & d6_{17} &= -8.6164088505538261656,\\
d6_8 &= 0.62695371915714817047, & d6_{18} &= 2.0586773175102798144,\\
d6_9 &= -0.055053822341965281964, & d6_{19} &= -0.17122615614350473339.
\end{aligned}
$$

The left boundary closure of the diagonal matrix $C_4^{(6)}$ is given by:

$$
\begin{bmatrix} 0 & 0 & 0 & 0 & 0 & 16.652411984262326459 & 1.1325448501150501650 & 1 & \cdots \end{bmatrix}.
$$

The corresponding right boundary closure is given by a permutation of both rows and columns. The left boundary closure of the diagonal matrix $C_5^{(6)}$ is given by:

$$\begin{bmatrix} 0 & 0 & 0 & 0 & 0 & 80.195967307267258036 & 1 & \cdots \end{bmatrix}.$$

The right boundary closure of the diagonal matrix $C_5^{(6)}$ is given by:

$$\begin{bmatrix} \cdots & 1 & 0 & 80.195967307267258036 & 0 & 0 & 0 & 0 & 0 \end{bmatrix}.$$

The left boundary closure of the diagonal matrix $C_6^{(6)}$ is given by:

$$\begin{bmatrix} 0 & 0 & 0 & 0 & 106.92521670797294276 & 11.429565737638910841 & 1 & \cdots \end{bmatrix}.$$

The corresponding right boundary closure is given by a permutation of both rows and columns.

The different $B^{(6)}$ matrices are given by

$$\begin{aligned} (B_4^{(6)})_{i,i} &= \frac{1}{3}(b_{i-1} + b_i + b_{i+1}) \\ (B_5^{(6)})_{i,i} &= \frac{1}{2}(b_i + b_{i+1}) \\ (B_6^{(6)})_{i,i} &= b_i \end{aligned} \quad .$$

The interior stencil of $M^{(b)}$ at row i is given by ($i = 10 \ldots N-9$):

$$\begin{aligned} m_{i,i-3} &= \frac{1}{40}b_{i-2} + \frac{1}{40}b_{i-1} - \frac{11}{360}b_{i-3} - \frac{11}{360}b_i \\ m_{i,i-2} &= \frac{1}{20}b_{i-3} - \frac{3}{10}b_{i-1} + \frac{1}{20}b_{i+1} + \frac{7}{40}b_i + \frac{7}{40}b_{i-2} \\ m_{i,i-1} &= -\frac{1}{40}b_{i-3} - \frac{3}{10}b_{i-2} - \frac{3}{10}b_{i+1} - \frac{1}{40}b_{i+2} - \frac{17}{40}b_i - \frac{17}{40}b_{i-1} \\ m_{i,i} &= \frac{1}{180}b_{i-3} + \frac{1}{8}b_{i-2} + \frac{19}{20}b_{i-1} + \frac{19}{20}b_{i+1} + \frac{1}{8}b_{i+2} + \frac{1}{180}b_{i+3} + \frac{101}{180}b_i \\ m_{i,i+1} &= -\frac{1}{40}b_{i-2} - \frac{3}{10}b_{i-1} - \frac{3}{10}b_{i+2} - \frac{1}{40}b_{i+3} - \frac{17}{40}b_i - \frac{17}{40}b_{i+1} \\ m_{i,i+2} &= \frac{1}{20}b_{i-1} - \frac{3}{10}b_{i+1} + \frac{1}{20}b_{i+3} + \frac{7}{40}b_i + \frac{7}{40}b_{i+2} \\ m_{i,i+3} &= \frac{1}{40}b_{i+1} + \frac{1}{40}b_{i+2} - \frac{11}{360}b_i - \frac{11}{360}b_{i+3} \end{aligned} \quad .$$

The left boundary closure of $M^{(b)}$ (given by a 9×9 matrix) is given by

$$
\begin{aligned}
m_{1,1} &= 0.7912667594695582093 9b_1 + 0.2968472090638000742 9b_2 \\
&\quad + 0.0031855190887964290152b_3 + 0.0163240404259095195 34b_4 \\
&\quad + 0.0316030224409441508 77b_5 + 0.0316796474801610529 96b_6 \\
&\quad + 0.0314857773394725392 05b_7, \\
m_{1,2} &= -1.0166893393503381444b_1 - 0.0284562737049161136 90b_3 \\
&\quad - 0.0412802983834929881 98b_4 - 0.1392281451620140507 5b_5 \\
&\quad - 0.1195777325611201766 6b_6 - 0.1194267756529333410 9b_7, \\
m_{1,3} &= 0.0707564293724371504 63b_1 - 0.1845476106024151050 3b_2 \\
&\quad - 0.0436416314711189234 70b_4 + 0.2432367907207732460 9b_5 \\
&\quad + 0.1582127073537215444 0b_6 + 0.1602348578364786307 6b_7, \\
m_{1,4} &= 0.2251991532891353212 7b_1 - 0.1662748711097054895 3b_2 \\
&\quad + 0.0271053096164867129 77b_3 - 0.1916646185968439909 1b_5 \\
&\quad - 0.0768411716019901459 44b_6 - 0.0821958694983169757 59b_7, \\
m_{1,5} &= -0.0522440346420205631 67b_1 + 0.0444006394850987622 10b_2 \\
&\quad - 0.0010239765473093878745b_3 + 0.0740348464531617409 05b_4 \\
&\quad + 0.0124162556899849689 54b_6 + 0.0718865284789260128 27b_5 \\
&\quad + 0.0137936299710473550 34b_7, \\
m_{1,6} &= -0.0182889681387719735 27b_1 + 0.0095746331632217580 607b_2 \\
&\quad - 0.0008105784530576404 2779b_3 - 0.0073488455877755196 984b_4 \\
&\quad + 0.0106360194972390699 70b_5 - 0.0131596703838261838 24b_6 \\
&\quad - 0.0211793647883875352 46b_7, \\
m_{1,7} &= 0.0019118885633161709274b_4 - 0.0406813035552914993 61b_5 \\
&\quad + 0.0131967498107374916 70b_6 + 0.0255726651812378367 63b_7, \\
m_{1,8} &= 0.0155965287113678576 40b_5 - 0.0064861841573315378 995b_6 \\
&\quad - 0.0091103445540363197401b_7, \\
m_{1,9} &= 0.0005593983696629863 0593b_6 - 0.0013848225351007963 723b_5 \\
&\quad + 0.0008254241654378100 6633b_7, \\
m_{2,2} &= 1.3063321571116676286b_1 + 0.2542001760457345743 5b_3 \\
&\quad + 0.1043897828092562609 5b_4 + 0.6672328021032112950 9b_5 \\
&\quad + 0.4681819359722749441 1b_6 + 0.4676415410195836920 1b_7, \\
m_{2,3} &= -0.0909141026999246460 49b_1 + 0.1103611313171476425 3b_4 \\
&\quad - 1.2903975449975188870b_5 - 0.6639605248735044787 1b_6 \\
&\quad - 0.6615974464005206184 2b_7,
\end{aligned}
$$

$$
\begin{aligned}
m_{2,4} &= -0.28935573956534316666b_1 - 0.24213200040645927216b_3 \\
&\quad + 1.18767025502803102 77b_5 + 0.39565981499041363328b_6 \\
&\quad + 0.38600489217558000007b_7, \\
m_{2,5} &= 0.06712774475803763989 0b_1 + 0.00914719268207563018 00b_3 \\
&\quad - 0.18721961430038080217b_4 - 0.13193585588531745301b_6 \\
&\quad - 0.48715757368119118874b_5 - 0.10475163122754481381b_7, \\
m_{2,6} &= 0.02349927974590068869 4b_1 + 0.00724090538356518131 64b_3 \\
&\quad + 0.01858378996391679448 7b_4 - 0.09289616133938676174 3b_5 \\
&\quad + 0.12235132704188076670b_6 + 0.11135203204362950339b_7, \\
m_{2,7} &= -0.00483479140644690759 06b_4 + 0.23106838326878204031b_5 \\
&\quad - 0.10807741421960079917b_6 - 0.11815617764273433354b_7, \\
m_{2,8} &= -0.08368141434403455353 7b_5 + 0.04093499466767054661 6b_6 \\
&\quad + 0.04274641967636400692 1b_7, \\
m_{2,9} &= -0.00357654513269698314 34b_6 + 0.00738939912412107868 21b_5 \\
&\quad - 0.00381285399142409553 87b_7, \\
m_{33} &= 0.00632716114713687380 78b_1 + 0.11473182007158685275b_2 \\
&\quad + 0.11667405542796800075b_4 + 2.76661080828544403 72b_5 \\
&\quad + 1.07092068996081710 42b_6 + 1.01316139103297305 72b_7, \\
m_{34} &= 0.02013769413884797246 6b_1 + 0.10337179946308864017b_2 \\
&\quad - 2.91322162115174272 43b_5 - 0.87558073434822622598b_6 \\
&\quad - 0.69099571834888124265b_7, \\
m_{35} &= -0.00467175109157546286 83b_1 - 0.02760353365637712827 8b_2 \\
&\quad - 0.19792902986208699745b_4 + 0.54029853383734330523b_6 \\
&\quad + 1.23917759303191107 79b_5 + 0.26280380502473582273b_7, \\
m_{36} &= -0.00163543086692188781 95b_1 - 0.00595247527588325961 97b_2 \\
&\quad + 0.01964682777744275219 4b_4 + 0.32366400126390466006b_5 \\
&\quad - 0.46595166932288709739b_6 - 0.22172727209417368594b_7, \\
m_{37} &= -0.00511135318935247454 96b_4 - 0.53558781637747543460b_5 \\
&\quad + 0.33283351044897389336b_6 + 0.20786565911785401579b_7, \\
m_{38} &= 0.18243281741342895622b_5 - 0.10598160301968184459b_6 \\
&\quad - 0.07645121439374711163 0b_7, \\
m_{39} &= 0.00920908996344379948 56b_6 - 0.01591502818872493167 1b_5 \\
&\quad + 0.00670593822528113218 53b_7,
\end{aligned}
$$

$$
\begin{aligned}
m_{44} &= 0.064092997759871869867b_1 + 0.093136576388046999489b_2 \\
&\quad + 0.230636762463474922291b_3 + 3.68944030828371662003b_5 \\
&\quad + 1.190550338687608873 8b_6 + 0.591247954688885651 94b_7, \\
m_{45} &= -0.014868958192656041286b_1 - 0.024870405993901607642b_2 \\
&\quad - 0.008712928907711754187 1b_3 - 1.263507837371824205 7b_6 \\
&\quad - 0.305831739784399732 69b_7 - 1.470691926045802954 8b_5, \\
m_{46} &= -0.005205147429855955657 6b_1 - 0.005363098747528542489 0b_2 \\
&\quad - 0.006897142765790609546 3b_3 - 0.785752452166745010 17b_5 \\
&\quad + 0.229114800542373460 01b_7 + 0.997706435629275052 92b_6, \\
m_{47} &= 0.669729748806766226 52b_5 - 0.501324735607212793 90b_6 \\
&\quad - 0.179516124310664543 73b_7, \\
m_{48} &= -0.202290906011175156 52b_5 + 0.145342185806365849 86b_6 \\
&\quad + 0.056948720204809306656b_7, \\
m_{49} &= -0.012004296184410038337b_6 - 0.004776915669385923 8415b_7 \\
&\quad + 0.016781211853795962179b_5, \\
m_{55} &= 0.003449455095910233625 2b_1 + 0.006641183499427826101 6b_2 \\
&\quad + 0.000329154508327186285 85b_3 + 0.335772170757647720 00b_4 \\
&\quad + 2.096413329579026439 0b_6 + 0.231732320418312685 50b_7 \\
&\quad + 0.006107825764368264576 5b_8 + 0.710912585068337669 56b_5, \\
m_{56} &= 0.001207544072304193806 1b_1 + 0.001432116665752147607 5b_2 \\
&\quad + 0.000260558264618325595 73b_3 - 0.033329411132516353908b_4 \\
&\quad - 0.280824169738553268 36b_7 - 0.027209080835250836084b_8 \\
&\quad + 0.104586543568292198 74b_5 - 1.348436986667115543 2b_6, \\
m_{57} &= 0.008671038084174692625 1b_4 + 0.173607341135542856 37b_6 \\
&\quad + 0.053313621252876254126b_8 - 0.242493526240452630 18b_5 \\
&\quad + 0.156901525767858827 06b_7, \\
m_{58} &= -0.086316839802171222760b_6 + 0.026988423604709992435b_7 \\
&\quad + 0.080981941477156510853b_5 - 0.032764636390806391639b_8, \\
m_{59} &= 0.007462059484530855073 3b_6 - 0.000812164036166867894 96b_7 \\
&\quad + 0.000552270208812709020 93b_8 - 0.007202165657176696199 3b_5, \\
m_{66} &= 0.000422722617344934504 25b_1 + 0.000308824194437896440 48b_2 \\
&\quad + 0.000206257570664743062 02b_3 + 0.003308343404200968256 7b_4 \\
&\quad + 0.582804701640500181 58b_5 + 0.805417422036621547 36b_7
\end{aligned}
$$

$$
\begin{aligned}
&+0.13383632334100334433b_8+0.00555555555555555555556b_9\\
&+1.1903620718618930511b_6,\\
m_{67}=&-0.000860704425268641330 26b_4-0.17480747086739049893b_5\\
&-0.31325448501150501650b_8-0.025000000000000000000b_9\\
&-0.31691663053104292713b_7-0.66916070916479291611b_6,\\
m_{68}=&\,0.033546617916933521087b_5-0.33436200223869714050b_7\\
&+0.050000000000000000000b_9+0.216979060980760275 08b_6\\
&+0.18383632334100334433b_8,\\
m_{69}=&\,0.029125184768230046430b_7+0.022790919164749163916b_8\\
&-0.030689859975187405305b_6-0.001781799513347360596 2b_5\\
&-0.030555555555555555556b_9,\\
m_{77}=&\,0.000223922237357715991790b_4+0.12754377854309566738b_5\\
&+1.011699483929608164 6b_6+0.969881727517257524 75b_8\\
&+0.125000000000000000000b_9+0.00555555555555555555556b_{i-3}\\
&+0.482317754303128150 01b_7,\\
m_{78}=&-0.037841139730330129499b_5-0.29975568851348273616b_6\\
&-0.300000000000000000000b_9-0.025000000000000000000b_{i-3}\\
&-0.39914868674468211784b_7-0.43825448501150501650b_8,\\
m_{79}=&\,0.046981462180226839339b_6-0.29668637874712374587b_8\\
&+0.050000000000000000000b_{i-3}+0.17163557041460064817b_7\\
&+0.003069346152296258362 4b_5+0.175000000000000000000b_9,\\
m_{88}=&\,0.012303289427168044554b_5+0.11836475296458983325b_6\\
&+0.941051189822794333 42b_7+0.950000000000000000000b_9\\
&+0.125000000000000000000b_{i-3}+0.00555555555555555555556b_{i-2}\\
&+0.569947434452114455 45b_8,\\
m_{89}=&-0.023080678926719163396b_6-0.29866250537751494972b_7\\
&-0.300000000000000000000b_{i-3}-0.025000000000000000000b_{i-2}\\
&-0.001047734860515050802 6b_5-0.42720908083525083608b_8\\
&-0.425000000000000000000b_9,\\
m_{99}=&\,0.005139370221149109977 0b_6+0.12477232150094220014b_7\\
&+0.950552270208812709 02b_8+0.950000000000000000000b_{i-3}\\
&+0.125000000000000000000b_{i-2}+0.00555555555555555555556b_{i-1}\\
&+0.000091593624651536418269b_5+0.561111111111111111111b_9.
\end{aligned}
$$

The corresponding right boundary closure is given by replacing $b_i \rightarrow b_{N+1-i}$ for $i = 1..12$ followed by a permutation of both rows and columns.

A.4 Eighth-order accurate

For the eighth order case, we did not manage to find boundary closures in $D^{(8)}_{5,6,7,8}$ and $C^{8}_{5,6,7,8}$ such that we get back the compatible narrow stencil SBP operator presented in [19]. This is not to say that such closure does not exist with the construction in (8). However, we are free to chose for example the difference operator $D^{(8)}_5$:

$$\begin{bmatrix} -1 & 5 & -10 & 10 & -5 & 1 & & \\ -1 & 5 & -10 & 10 & -5 & 1 & & \\ -1 & 5 & -10 & 10 & -5 & 1 & & \\ & -1 & 5 & -10 & 10 & -5 & 1 & \\ & & \ddots & \ddots & \ddots & \ddots & \ddots & \ddots \end{bmatrix},$$

the difference operator $D^{(8)}_6$:

$$\begin{bmatrix} 1 & -6 & 15 & -20 & 15 & -6 & 1 & \\ 1 & -6 & 15 & -20 & 15 & -6 & 1 & \\ 1 & -6 & 15 & -20 & 15 & -6 & 1 & \\ 1 & -6 & 15 & -20 & 15 & -6 & 1 & \\ & 1 & -6 & 15 & -20 & 15 & -6 & 1 \\ & & \ddots & \ddots & \ddots & \ddots & \ddots & \ddots \end{bmatrix},$$

the difference operator $D^{(8)}_7$:

$$\begin{bmatrix} 1 & -6 & 15 & -20 & 15 & -6 & 1 & & \\ -1 & 7 & -21 & 35 & -35 & 21 & -7 & 1 & \\ -1 & 7 & -21 & 35 & -35 & 21 & -7 & 1 & \\ -1 & 7 & -21 & 35 & -35 & 21 & -7 & 1 & \\ & -1 & 7 & -21 & 35 & -35 & 21 & -7 & 1 \\ & & \ddots & \ddots & \ddots & \ddots & \ddots & \ddots & \end{bmatrix},$$

and the difference operator $D_8^{(8)}$:

$$\begin{bmatrix} 1 & -6 & 15 & -20 & 15 & -6 & 1 & & & \\ 1 & -8 & 28 & -56 & 70 & -56 & 28 & -8 & 1 & \\ 1 & -8 & 28 & -56 & 70 & -56 & 28 & -8 & 1 & \\ 1 & -8 & 28 & -56 & 70 & -56 & 28 & -8 & 1 & \\ 1 & -8 & 28 & -56 & 70 & -56 & 28 & -8 & 1 & \\ & 1 & -8 & 28 & -56 & 70 & -56 & 28 & -8 & 1 \\ & & \ddots & \ddots & \ddots & \ddots & \ddots & \ddots & \ddots & \end{bmatrix}.$$

Based on the closures in the corresponding 4th and 6th order cases an initial guess is to set the first 6–8 points to zero in $C^8_{5,6,7,8}$ to zero to get a closure not to bad.

At least we know how to chose the diagonal matrices $B^{(8)}_{5,6,7,8}$ in (8) to obtain a narrow interior stencil:

$$\begin{aligned} (B_5^{(8)})_{i,i} &= \frac{1}{4}(b_{i-1} + b_i + b_{i+1} + b_{i+2}) \\ (B_6^{(8)})_{i,i} &= \frac{3}{10}\left(b_{i-1} + \frac{4}{3}b_i + b_{i+1}\right) \\ (B_7^{(8)})_{i,i} &= \frac{1}{2}(b_i + b_{i+1}) \\ (B_8^{(8)})_{i,i} &= b_i \end{aligned}.$$

at $i = 1..N-2$. Since $B^{(8)}_{5,6,7,8}$ are multiplied with $C^8_{5,6,7,8}$ that are zero at the first few boundary points, we can as well put the corner points to zero in $B^{(8)}_{5,6,7,8}$.

This means that to the interior stencil of $M^{(b)}$ at row i is given by ($i = 13 \ldots N-12$):

$$\begin{aligned} m_{i,i-4} &= -\frac{1}{280}b_{i-2} - \frac{1}{210}b_{i-3} - \frac{1}{210}b_{i-1} + \frac{5}{672}b_{i-4} + \frac{5}{672}b_i, \\ m_{i,i-3} &= \frac{2}{35}b_{i-2} + \frac{2}{35}b_{i-1} - \frac{1}{70}b_{i-4} - \frac{1}{70}b_{i+1} - \frac{1}{18}b_{i-3} - \frac{1}{18}b_i, \\ m_{i,i-2} &= \frac{11}{105}b_{i-3} - \frac{2}{5}b_{i-1} + \frac{3}{280}b_{i-4} + \frac{3}{280}b_{i+2} + \frac{11}{105}b_{i+1} + \frac{31}{168}b_{i-2} + \frac{31}{168}b_i, \\ m_{i,i-1} &= -\frac{13}{35}b_{i-2} - \frac{1}{15}b_{i-3} - \frac{1}{210}b_{i-4} - \frac{1}{15}b_{i+2} - \frac{13}{35}b_{i+1} - \frac{1}{210}b_{i+3} - \frac{5}{14}b_{i-1} - \frac{5}{14}b_i, \end{aligned}$$

$$m_{i,i} = \frac{1}{1120}b_{i+4} + \frac{53}{280}b_{i-2} + \frac{17}{630}b_{i-3} + \frac{69}{70}b_{i-1} + \frac{1}{1120}b_{i-4} + \frac{53}{280}b_{i+2} + \frac{69}{70}b_{i+1} + \frac{17}{630}b_{i+3} + \frac{445}{1008}b_i,$$

$$m_{i,i+1} = -\frac{1}{210}b_{i+4} - \frac{1}{15}b_{i-2} - \frac{1}{210}b_{i-3} - \frac{13}{35}b_{i-1} - \frac{13}{35}b_{i+2} - \frac{1}{15}b_{i+3} - \frac{5}{14}b_{i+1} - \frac{5}{14}b_i,$$

$$m_{i,i+2} = \frac{3}{280}b_{i+4} + \frac{3}{280}b_{i-2} + \frac{11}{105}b_{i-1} - \frac{2}{5}b_{i+1} + \frac{11}{105}b_{i+3} + \frac{31}{168}b_{i+2} + \frac{31}{168}b_i,$$

$$m_{i,i+3} = -\frac{1}{70}b_{i+4} - \frac{1}{70}b_{i-1} + \frac{2}{35}b_{i+2} + \frac{2}{35}b_{i+1} - \frac{1}{18}b_i - \frac{1}{18}b_{i+3},$$

$$m_{i,i+4} = -\frac{1}{280}b_{i+2} - \frac{1}{210}b_{i+1} - \frac{1}{210}b_{i+3} + \frac{5}{672}b_{i+4} + \frac{5}{672}b_i.$$

References

1. Appelö, D., Petersson, N.A.: A stable finite difference method for the elastic wave equation on complex geometries with free surfaces. J. Comput. Phys. **5**, 84–107 (2009)
2. Bamberger, A., Glowinski, R., H Tran, Q.: A domain decomposition method for the acoustic wave equation with discontinuous coefficients and grid change. SIAM J. Numer. Anal. **34**(2), 603–639 (1997)
3. Calabrese, G.: Finite differencing second order systems describing black holes. Phys. Rev. D, Part. Fields **71**, 027501 (2005)
4. Carpenter, M.H., Gottlieb, D., Abarbanel, S.: Time-stable boundary conditions for finite-difference schemes solving hyperbolic systems: methodology and application to high-order compact schemes. J. Comput. Phys. **111**(2), 220–236 (1994)
5. Cohen, G., Joly, P.: Construction and analysis of fourth-order finite difference schemes for the acoustic wave equation in nonhomogeneous media. SIAM J. Numer. Anal. **33**(4), 1266–1302 (1996)
6. Grote, M., Schneebeli, A., Schötzau, D.: Discontinuous Galerkin finite element method for the wave equation. SIAM J. Numer. Anal. **44**, 2408–2431 (2006)
7. Grote, M., Schneebeli, A., Schötzau, D.: Interior penalty discontinuous Galerkin method for Maxwell's equations: energy norm error estimates. J. Comput. Appl. Math. **204**, 375–386 (2007)
8. Gustafsson, B.: The convergence rate for difference approximations to general mixed initial boundary value problems. SIAM J. Numer. Anal. **18**(2), 179–190 (1981)
9. Gustafsson, B., Kreiss, H.-O., Oliger, J.: Time dependent problems and difference methods. Wiley, New York, (1995)
10. Gustafsson, B., Wahlund, P.: Time compact difference methods for wave propagation in discontinuous media. SIAM J. Sci. Comput. **26**, 272–293 (2004)
11. Kamakoti, R., Pantano, C.: High-order narrow stencil finite-difference approximations of second-order derivatives involving variable coefficients. SIAM J. Sci. Comput. **31**(6), 4222–4243 (2009)
12. Kelly, K.R., Ward, R.W., Treitel, S., Alford, R.M.: Synthetic seismograms: a finite difference approach. Geophysics **41**, 2–27 (1976)
13. Kreiss, H.-O., Petersson, N.A., Ystrom, J.: Difference approximations for the second order wave equation. SIAM J. Numer. Anal. **40**, 1940–1967 (2002)
14. Lele, S.K.: Compact finite difference schemes with spectral-like resolution. J. Comput. Phys. **103**, 16–42 (1992)
15. Mattsson, K., Carpenter, M.H.: Stable and accurate interpolation operators for high-order multi-block finite-difference methods. SIAM J. Sci. Comput. **32**(4), 2298–2320 (2010)
16. Mattsson, K., Ham, F., Iaccarino, G.: Stable and accurate wave propagation in discontinuous media. J. Comput. Phys. **227**, 8753–8767 (2008)
17. Mattsson, K., Nordström, J.: Summation by parts operators for finite difference approximations of second derivatives. J. Comput. Phys. **199**(2), 503–540 (2004)
18. Mattsson, K., Svärd, M., Nordström, J.: Stable and accurate artificial dissipation. J. Sci. Comput. **21**(1), 57–79 (2004)

19. Mattsson, K., Svärd, M., Shoeybi, M.: Stable and accurate schemes for the compressible Navier-Stokes equations. J. Comput. Phys. **227**(4), 2293–2316 (2008)
20. Nordström, J., Carpenter, M.H.: Boundary and interface conditions for high-order finite-difference methods applied to the Euler and Navier-Stokes equations. J. Comput. Phys. **148**, 341–365 (1999)
21. Nycander, J.: Tidal generation of internal waves from a periodic array of steep ridges. J. Fluid Mech. **567**, 415–432 (2006)
22. Shubin, G.R., Bell, J.B.: A modified equation approach to constructing fourth order methods for acoustic wave propagation. SIAM J. Sci. Stat. Comput. **8**(2), 135–151 (1987)
23. Svärd, M.: On coordinate transformation for summation-by-parts operators. J. Sci. Comput. **20**(1), 29–42 (2004)
24. Svärd, M., Carpenter, M.H., Nordström, J.: A stable high-order finite difference scheme for the compressible Navier–Stokes equations, far-field boundary conditions. J. Comput. Phys. **225**, 1020–1038 (2008)
25. Svärd, M., Carpenter, M.H., Nordström, J.: A stable high-order finite difference scheme for the compressible Navier–Stokes equations, no-slip wall boundary conditions. J. Comput. Phys. **227**, 4805–4824 (2008)
26. Svärd, M., Mattsson, K., Nordström, J.: Steady-state computations using summation-by-parts operators. J. Sci. Comput. **24**(1), 79–95 (2005)
27. Svärd, M., Nordström, J.: On the order of accuracy for difference approximations of initial-boundary value problems. J. Comput. Phys. **218**, 333–352 (2006)
28. Szilagyl, B., Kreiss, H.-O., Winicour, J.W.: Modeling the black hole excision problem. Phys. Rev. D, Part. Fields **71**, 104035 (2005)
29. Virieux, J.: Sh-wave propagation in heterogeneous media: Velocity-stress finite-difference method. Geophysics **49**, 1933–1957 (1984)
30. Virieux, J.: P-sv wave propagation in heterogeneous media: velocity-stress finite-difference method. Geophysics **51**, 889–901 (1986)
31. Yee, K.S.: Numerical solution of initial boundary value problems involving maxwell's equations in isotropic media. IEEE Trans. Antennas Propag. **14**, 302–307 (1966)